

Platinum or nickel nanoparticles decorated on silica spheres by microwave irradiation technique

Ayşe BAYRAKÇEKEN*

Department of Chemical Engineering, Faculty of Engineering, Atatürk University, Erzurum, Turkey

Received: 08.06.2013 • Accepted: 26.09.2013 • Published Online: 14.03.2014 • Printed: 11.04.2014

Abstract: Supported catalysts are of great interest because of their wide range of application possibilities. In this study, firstly silica spheres were synthesized and then platinum and nickel nanoparticles were incorporated on this silica by microwave irradiation, which is an efficient technique for catalyst preparation. Synthesized silica spheres and catalysts were characterized by BET, X-ray diffraction, Fourier transform infrared spectroscopy, thermogravimetric analysis, and transmission electron microscopy techniques. Pt or Ni nanoparticles well dispersed over silica support were obtained using microwave irradiation.

Key words: Silica, microwave irradiation, supported catalyst, Pt/SiO₂, Ni/SiO₂

1. Introduction

Supported catalysts have a wide range of applications in different fields. Support materials used in catalysis produce high surface area and better dispersion of the catalyst material. Commonly used catalyst supports are carbon-based ones,^{1,2} alumina,³ zeolite,⁴ and silica.⁵ Of these supporting materials, silica has a potential to be used in a vast field of applications ranging from microelectronics to medical applications.⁶ The transition metals, including Pt and Ni, are very important in catalysis because of their catalytic activity for various reactions such as oxidation and reduction reactions.⁷

Supported catalysts can be prepared in 2 stages. Firstly, the metal salt is dispersed over the support material and then the supported metal salt is converted to its metallic form. The first step can be achieved by means of different techniques, including impregnation, precipitation, or deposition, while the second step includes calcination or reduction.⁸ These 2 steps significantly affect the properties of the catalyst, which have to be handled carefully. Among the other catalyst preparation techniques, microwave irradiation is growing in popularity because it is a time saving and energy efficient process.⁹ In this technique, it is important to use a material that has the ability to absorb the microwave power and then convert it to heat efficiently. This property of the chemical used in the synthesis is related to the material's loss factor or loss tangent.¹⁰ Ethylene glycol (EG), frequently used in microwave irradiation, has a high loss tangent of 1.35 at 2.45 GHz, which is a high value when compared to other solvents.⁹ EG used in this process not only serves as the reducing agent but also provides the heating environment.

Silica-supported catalysts can be prepared by using water-in-oil type microemulsion,¹¹ and template synthesis of Pt over silica nanoparticles.¹² Ni nanoparticles were synthesized on the walls of microporous silica

*Correspondence: ayse.bayrakceken@gmail.com

spheres.¹³ Unsupported Ni nanoparticles,¹⁴ carbon-supported Pt,¹⁵ and silica aerogel-supported Pt¹⁶ were successfully synthesized by microwave irradiation. In the present study, firstly production of spherical silica was achieved and then Pt or Ni nanoparticles were impregnated over this support material by microwave irradiation. It was aimed to produce highly dispersed nanoparticles over the silica support.

2. Experimental

Silica spherical particles were produced as described previously.⁶ Briefly, 1.0 g of cetyl trimethylammonium bromide (CTAB, Merck) and 0.6 g of urea (Doğa İlaç) were dissolved in 30 mL of water. Then 2.5 g of tetraethyl orthosilicate (TEOS, Acros) was dissolved in 30 mL of cyclohexane (Merck) and 1 mL of isopropanol (Merck). Both solutions were mixed while being vigorously stirred. This mixture was stirred at room temperature for 30 min, and then the temperature was increased to 70 °C and the mixture was kept at this temperature overnight. The resultant material was centrifuged, and washed with acetone and water several times. The precipitate was then put into 50 mL of ethanol and in order to remove the surfactant 4 mL of 12 M HCl was added under stirring at 70 °C for 3 h.

Pt/silica catalysts were prepared by microwave heating of EG solutions of the Pt and Ni precursors as described elsewhere.¹⁷ Briefly, the required volume of 0.05 M aqueous solutions of Pt precursor (H_2PtCl_6) or Ni precursor ($\text{Ni}(\text{NO}_3)_2$) and 50 mL of EG were mixed in a beaker. Then 0.1 g silica, 0.1 M NaOH and CTAB were added to this solution. After ultrasonication for 30 min, the mixture was put in a microwave oven and heated for 60 s at 800 W microwave power. The resulting suspension was cooled immediately, and then filtered and the residue was washed with acetone. The solid product was dried at 100 °C overnight in a vacuum oven.

The produced silica and supported catalysts were characterized by using BET, X-ray diffraction (XRD), Fourier transform infrared (FTIR) spectroscopy, thermogravimetric analysis (TGA), and transmission electron microscopy (TEM). Nitrogen adsorption–desorption analyses were carried out by a Quantachrome Autosorb-1-C/MS instrument. Multipoint BET surface area, pore size distribution, and pore volume of the silica were analyzed by this technique. XRD data were obtained by a Rigaku Miniflex X-ray diffractometer. The IR spectra of the materials were recorded using a PerkinElmer Spectrum One FT-IR spectrometer. Thermogravimetric analyses of the materials were achieved using a Netzsch thermal analyzer by heating the samples in flowing air from room temperature to 1000 °C at a heating rate of 10 °C/min. A JEOL JEM 2100F STEM instrument was used for TEM analysis.

3. Results and discussion

The nitrogen adsorption/desorption and pore size distribution of the synthesized silica is shown in Figures 1(a) and (b), respectively, and the results obtained from these data are given in the Table. A silica material with a large surface area (430.8 m²/g) was obtained. The produced silica has a BJH pore volume of 0.5905 cc/g and a BJH pore diameter of 3.05 nm. Nitrogen adsorption-desorption isotherm is of type IV, which indicates formation of a mesoporous structure and its hysteresis loop is of H4 type.

Table. Structural parameters of silica.

Multipoint BET surface area (m ² /g)	BJH pore diameter (nm)	BJH pore volume (cc/g)
430.8	3.05	0.5905

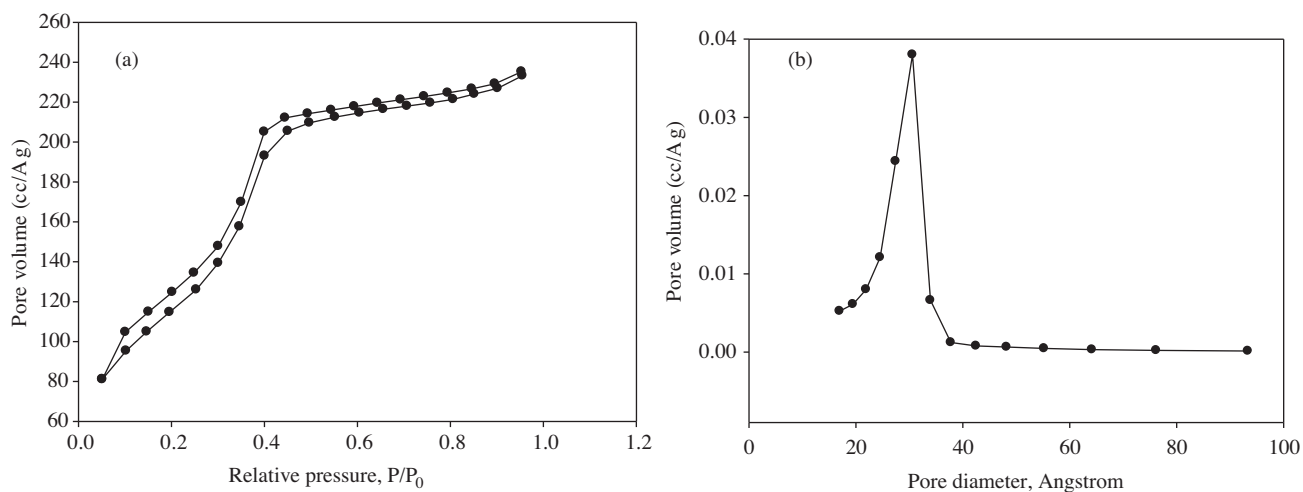


Figure 1. a) Nitrogen adsorption/desorption isotherm of silica b) pore size distribution of silica.

Figure 2 shows the XRD pattern of the produced silica and the supported catalysts. The silica showed an amorphous structure. The characteristic peaks of (111), (200), (220) and (311) corresponding to the Pt were observed.¹⁸ A broad peak located at 1530° (angle of 2θ) confirms the amorphous nature of the silica.¹⁹ The corresponding peaks for Ni nanoparticles were not so clear. There was a small peak corresponding to fcc (111) Ni phase located at around 45° .

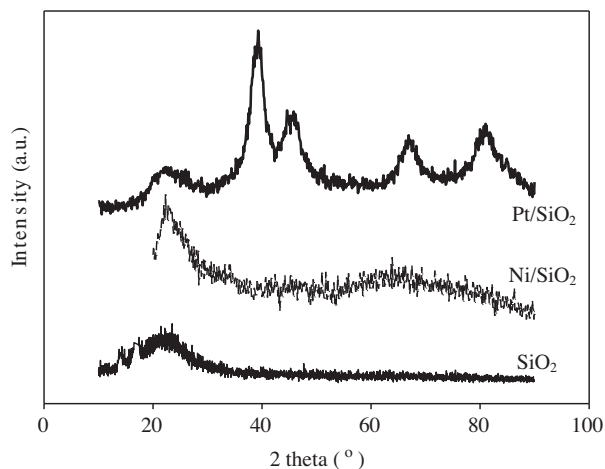


Figure 2. XRD pattern for silica and supported catalysts.

FTIR spectra of the silica and prepared catalysts are given in Figure 3. In the FTIR spectrum an absorption band representing the asymmetric stretching vibration of siloxane (SiOSi) (1095 cm^{-1}) was observed, which shows the movement of the bridging oxygen atom to the SiSi lines in the opposite direction to their Si neighbors.^{20,21} The band at about 467 cm^{-1} corresponds to SiO rocking vibration where the oxygen atom moves perpendicular to the SiOSi plane.²² The band at 967 cm^{-1} shows asymmetric vibration of SiOH.³ The bands located at 2853.97 , 2854.28 , and 2854.53 cm^{-1} correspond to CH stretching and those at 2924.90 , 2925.64 , and 2925.97 cm^{-1} correspond to (CH_2) for the presence of unreacted TEOS in silica particles for

SiO_2 , Pt/SiO_2 , and Ni/SiO_2 , respectively; the values were shifted to higher wavenumbers for the supported catalysts.³ The intensity of the bands decreased for the supported catalysts and the smallest one was for Pt/SiO_2 . The absorption bands between 3300 and 3500 cm^{-1} correspond to OH stretching in H-bonded water, which can be also checked with the bending vibration (scissoring) of molecular water at 1635 cm^{-1} . The intensity of the bands associated with water increased for Ni/SiO_2 catalyst. The bands located between 800 and 1260 cm^{-1} correspond to various SiO_2 peaks, SiOH bonding, and the residual organic compounds left in the structure.²³ The FTIR spectrum shows the characteristics of silica when compared to the literature.

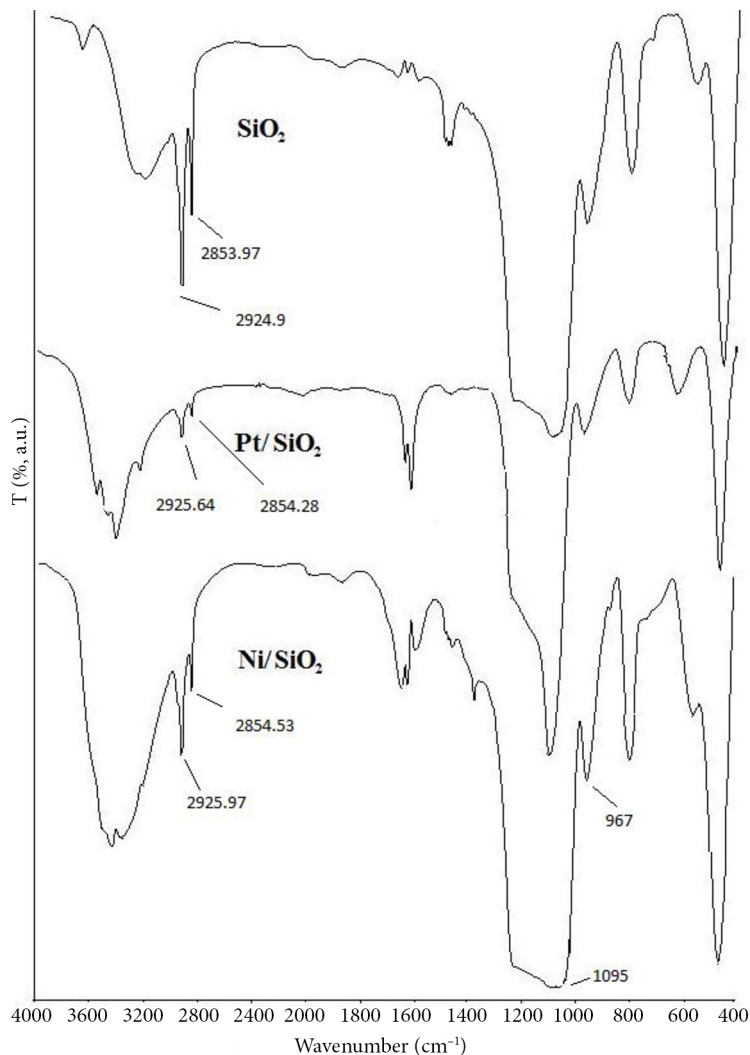


Figure 3. FTIR spectra for silica and supported catalysts.

TGA analysis has been used to determine the metal loading over silica support. In Figure 4, TGA results for untreated silica and silica treated with microwave (a), and TGA and DTG results for (b) silica treated with microwave, (c) Pt/SiO_2 , and (d) Ni/SiO_2 are shown. The supported catalysts were prepared using microwave irradiation. In order to determine the change in the structure the blank silica material was exposed to microwave radiation in EG having the same conditions as that of the supported catalysts prepared. It was observed that there was a huge difference between the untreated and treated silica materials. In the light of this observation,

the metal loading over the silica material was determined by comparing the supported catalysts with the treated silica. The Pt loading and Ni loading over the silica were obtained as 24.2% and 17.2%, respectively. The DTG curves show sharp peaks from room temperature to 700 °C, which can be attributed to the loss of physically adsorbed water from the silica surface between 30 and 500 °C,²⁴ and chemically adsorbed water bonded to SiOH with the hydrogen bond.²⁵ Thermal degradation of pure CTAB shows a mass loss in the temperature range of 180-340 °C as seen for all the samples.¹⁸ The small peaks occurring between 500 and 1000 °C can be attributed to the further degradation of the surfactant.¹⁸

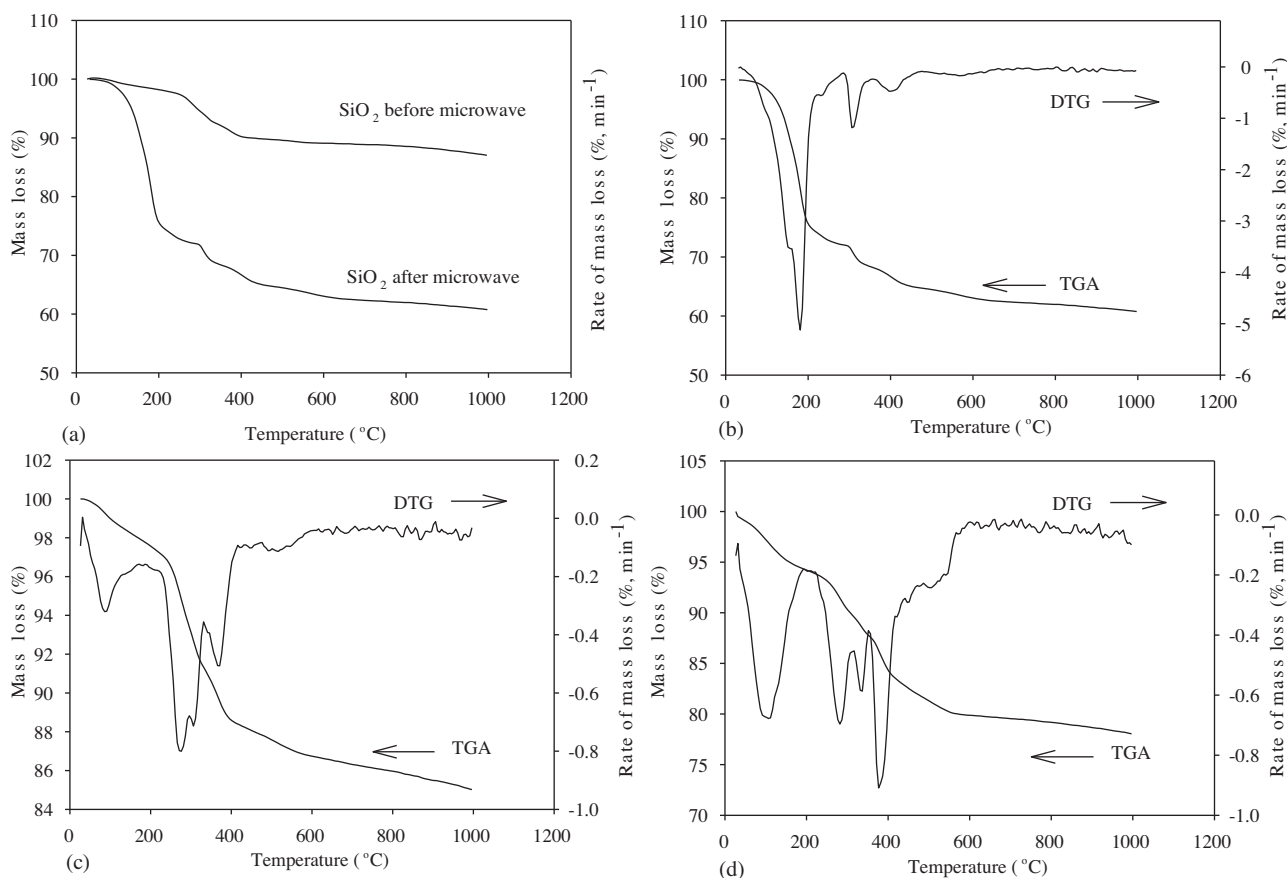


Figure 4. a) TGA results for untreated silica and silica treated with microwave and TGA and DTG results for b) silica treated with microwave c) Pt/Si SiO₂ d) Ni/Si SiO₂.

In Figure 5, TEM images of the silica [(a)(d)], Pt/Si SiO₂ [(e)(h)], and Ni-Si SiO₂ [(i) and (j)] are given. Spherical silica particles having a porous structure were obtained. It was seen that Pt and Ni nanoparticles were decorated on silica mostly homogeneously but for Pt/Si SiO₂ catalyst there were some agglomerated particles. The distribution of the nanoparticles in Ni/Si SiO₂ catalyst was more homogeneous. The structure of the support in the supported catalysts is a key parameter that affects the distribution of the nanoparticles. Utilization of CTAB as surfactant resulted in the prevention of agglomeration of the nanoparticles. TEM results were used to determine the particle sizes of the catalysts. Pt and Ni particle sizes were obtained as 2.8 and 3.3 nm, respectively.

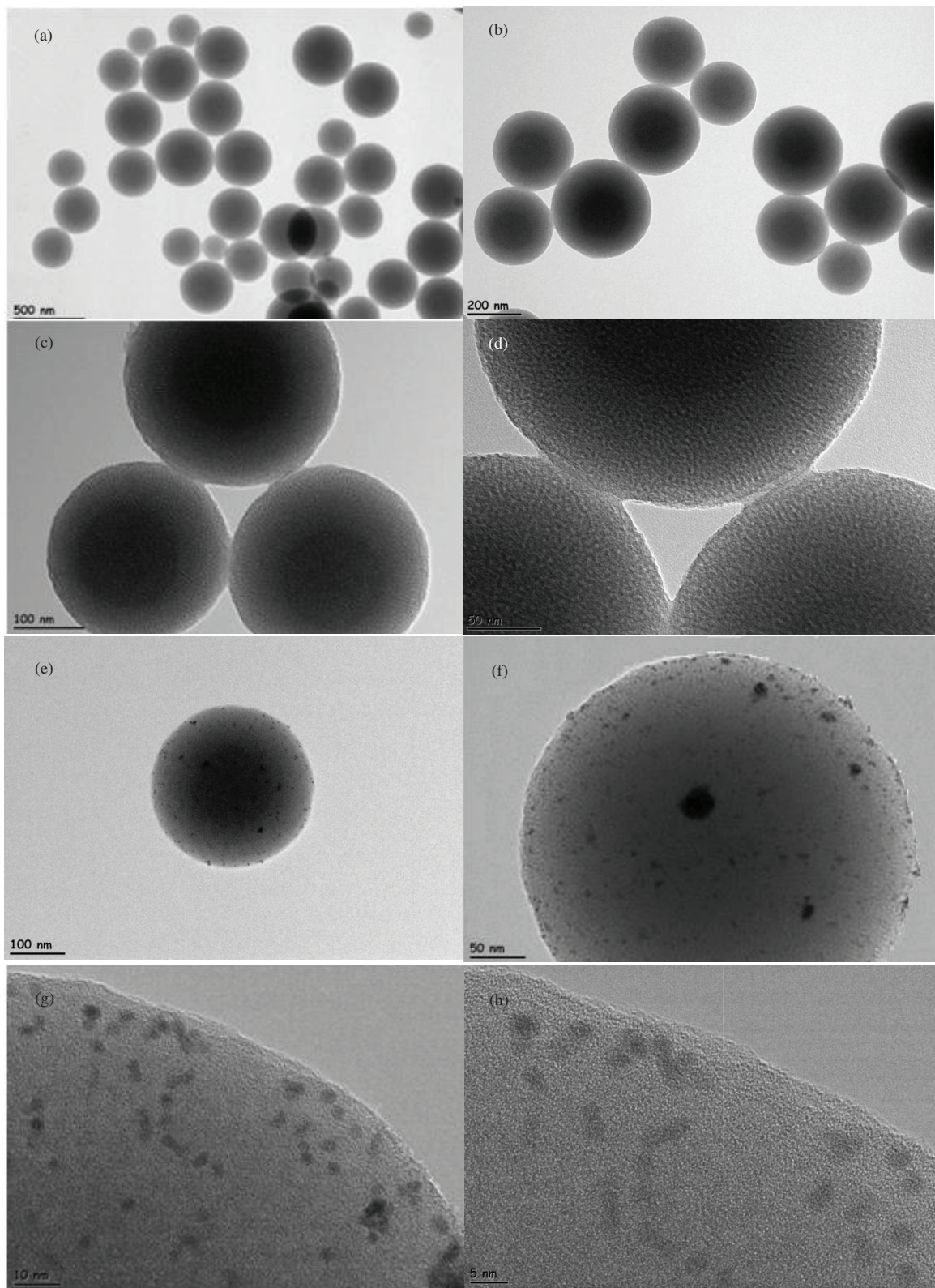


Figure 5. TEM images of (a)–(d) SiO₂, (e)–(h) Pt/SiO₂, (i) and (j) Ni/SiO₂.

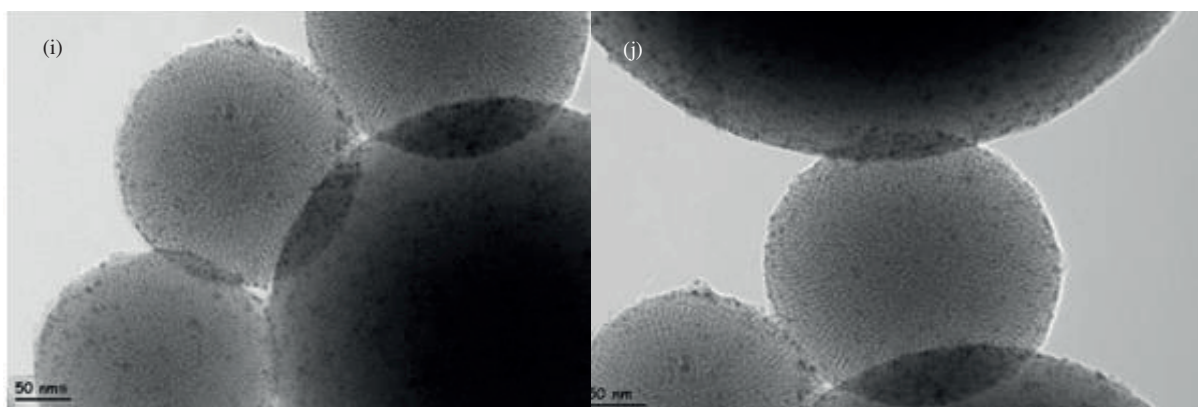


Figure 5. Continued.

The spherical silica particles having high surface area were synthesized. There was a significant difference in the silica material after microwave treatment and so some additional treatments after the synthesis of silica material can be applied in order to obtain much purer material. Decoration of Pt and Ni nanoparticles on the spherical silica was achieved using microwave irradiation. This process is a fast, efficient, and simple way of catalyst preparation. Some agglomerated particles occurred during the preparation process, which can be reduced by increasing the amount of surfactant used and by optimizing the conditions of catalyst preparation.

Acknowledgments

The author gratefully acknowledges the financial support of Atatürk University BAP projects through grant numbers 2009/256 and 2011/144. Dr Hatice Bayrakçeken is gratefully acknowledged for the TGA analysis.

References

1. Jia, R. L.; Wang, C. Y.; Wang, S. M. *J. Mater. Sci.* **2006**, *41*, 6881–6888.
2. Planeix, J. M.; Coustel, N.; Coq, B.; Brotons, V.; Kumbhar, P. S.; Dutartre R.; Geneste, P.; Bernier, P.; Ajayan, P. M. *J. Am. Chem. Soc.* **1994**, *116*, 7935–7936.
3. Li, Z. X.; Shi, F. B.; Li, L. L.; Zhang, T.; Yan, C. H. *Phys. Chem. Chem. Phys.* **2011**, *13*, 2488–2491.
4. Ogino, I.; Chen, C. Y.; Gates, B. C. *Dalton Trans.* **2010**, *39*, 8423–8431.
5. Min, B. K.; Santra, A. K.; Goodman, D. W. *Catal. Today* **2003**, *85*, 113–124.
6. Moon, D. S.; Lee, J. K. *Langmuir* **2012**, *28*, 12341–12347.
7. Travitsky, N.; Ripenbein, P.; Golodnitsky, D.; Rosenberg, Y.; Burshtein, L.; Peled, E. *J. Power Sources* **2006**, *161*, 782–789.
8. Farrukh, M. A.; Heng, B. T.; Adnan, R. *Turk. J. Chem.* **2010**, *34*, 537–550.
9. Bayrakçeken, A.; Türker, L.; Eroğlu, İ. *Int. J. Hydrogen Energ.* **2008**, *33*, 7527–7537.
10. Tierney, J. P.; Lidström, P. *Microwave Assisted Organic Synthesis*; CRC Press: Boca Raton, FL, USA, 2005.
11. Hori, K.; Matsune, H.; Takenaka, S.; Kishida, M. *Sci. Tech. Adv. Mater.* **2006**, *7*, 678–684.
12. Li, A.; Zhao, J. X.; Pierce, D. T. *J. Colloid Interface Sci.* **2010**, *351*, 365–371.
13. Godsell, J. F.; Donegan, K. P.; Tobin, J. M.; Copley, M. P.; Rhen, F. M. F.; Otway, D. J.; Morris, M. A.; O'Donnell, T.; Holmes, J. D.; Roy, S. *J. Magn. Magn. Mater.* **2010**, *322*, 1269–1274.
14. Xu, W.; Liew, K. Y.; Liu, H.; Huang, T.; Sun, C.; Zhao, Y. *Mater. Lett.* **2008**, *62*, 2571–2573.

15. Song, S.; Liu, J.; Shi, J.; Liu, H.; Maragou, V.; Wang, Y.; Tsiakaras, P. *Appl. Catal. B Environ.* **2011**, *103*, 287–293.
16. Tsai, C. H.; Yang, F. L.; Chang, C. H.; Chen-Yang, Y. W. *Int. J. Hydrogen Energ.* **2012**, *37*, 7669–7676.
17. Liu, Z.; Gan, L. M.; Hong, L.; Chen, W.; Lee, J. Y. *J. Power Sources* **2005**, *139*, 73–78.
18. Fıçıcılar, B.; Bayrakçeken, A.; Eroğlu, İ. *Int. J. Hydrogen Energ.* **2010**, *35*, 9924–9933.
19. Ramesh, S.; Kolytyn, Y.; Prozorov, R.; Gedanken, A. *Chem. Mater.* **1997**, *9*, 546–551.
20. Singho, N. D.; Johan, M. R. *Int. J. Electrochem. Sci.* **2012**, *7*, 5604–5615.
21. Wang, W.; Song, M.; Zhang, Z. Y.; Richardson, M. J. *Non-Cryst. Solids* **2006**, *352*, 2180–2186.
22. Hernandez, C.; Pierre, A. C. *Langmuir* **2000**, *16*, 530–536.
23. Beganskienė, A.; Sirutkaitis, V.; Kurtinaitienė, M.; Juškėnas, R.; Kareiva, A. *Mater. Sci. (Medžiagotyra)* **2004**, *10*, 287–290.
24. Ramimoghadam, D.; Bin Hussein, M. Z.; Taufiq-Yap, Y. H. *Int. J. Mol. Sci.* **2012**, *13*, 13275–13293.
25. Liu, K.; Feng, Q.; Yang, Y.; Zhang, G.; Ou, L.; Lu, Y. *J. Non-Cryst. Solids* **2007**, *353*, 1534–1539.